Energy harvesting in a fluid flow using piezoelectric materials

M. Curatolo[1], M. La Rosa[1], P. Prestininzi[1]
[1]University of Roma Tre, Engineering Department, Rome, Italy

Abstract

We present a model able to estimate electrical energy generated by a deformable piezoelectric solid immersed in a fluid flow. This problem involves different physics: solid mechanics, fluid mechanics, electrostatics and an appropriate electrical load resistance capable to harvest the electrical energy developed by the deformation of a piezoelectric material immersed in a fluid flow. The interaction between different fields of physics makes the problem complex and highly nonlinear. In our case, since the solid exhibits large deformations, simulate energy harvesting in a fluid flow requires multiphysics and a deeply use of advanced features of COMSOL.

Keywords: energy harvesting, piezoelectric materials, fluid-solid interaction.

Introduction

Energy harvesting using piezoelectric materials has been deeply studied over the last decade [1, 2, 3]. This technology provides extra sources of electric power which can be used to recharge electronic devices with a limited battery duration. The concept has ecological implications in reducing the chemical waste produced by replacing batteries and monetary gains by reducing maintenance costs. For this reason and not only, in the last years the area of energy harvesting has attracted academic and industry. One of the most studied areas is the use of the piezoelectric effect to convert ambient vibration into useful electrical energy. An example of such application is the energy harvesting through piezoelectric materials in a flowing fluid [4, 5]. Fluid flow has the potential to provide significant mechanical energy input for piezoelectric harvesters. However, the efficient conversion of the bulk kinetic energy of a steady and uniform flow into time-dependent elastic energy in the piezoelectric structure remains a significant challenge. The modeling of such multiphysics problem has still to be fully investigated and requires advanced numerical tools which can be tackled with COMSOL Multiphysics.

In this work, we focus on the generation of electrical power through a piezoelectric solid immersed in a channel using an inverted configuration of the solid with respect to the flow, similarly to [5]. The solid is a non-homogeneous bilayer solid, clamped at one end on a fixed circular constraint. The solid is composed of two layers; one is piezoelectric (PZT 5-A) while the other has a structural function and enables the generation of electrical power by the piezoelectric layer. In this model, we use the fluid-structure interaction (FSI) package of COMSOL together with the electrostatics and electric circuit packages. In particular, large deformations of the solid are effectively described through the moving mesh and the remeshing features of COMSOL as in [6, 7]. The advantage of numerical simulations easily allows parametric studies for different sizes of the half cylinder and for different inlet velocities to optimize the energy harvesting device. Finally, it is worth noting that in this problem the multiphysics approach is necessary as some relevant informations about the energy harvesting just arise by the coupling between different physics.

Model and Theory

The problem is solved in a bi-dimensional (2D) space using a orthonormal reference frame (o, $\mathbf{e}_1$, $\mathbf{e}_2$) and coordinates (X,Y), with o the origin and $\mathbf{e}_1$ leaning on the horizontal axis of symmetry of the channel. The computational domain Ω is the union of a solid domain Ω_s, assumed as reference configuration, and a mesh domain Ω_m, (see, Fig. 1) which represents the domain occupied by the fluid at any instant t of the time interval $\mathscr{T}$. In particular, the solid domain is composed of a piezoelectric solid Ω_{sp} which, when deformed, develops an electrical field and a structural solid Ω_{ss} which has a half cylinder shape to improve vibrations and does not generate any electrical field. The balance equations for the solid are written with respect to Ω_s (material, or Lagrangian formulation), while those for the fluid are written with respect to Ω_m (Arbitrary Eulerian-Lagrangian (ALE) formulation [8]). The channel has height H and length L, the piezoelectric solid has a length L_p and thickness h_p, and the structural solid has length L_s and thickness h_s. Both solids are clamped to a circular fixed constraint of diameter D (the white colored circle in Fig. 1). State variables of the model are the material vector field $\mathbf{u}_s$, describing the displacement of the solid, the vector field $\mathbf{v}_f$, representing the velocity of the fluid, the material scalar field V, describing the electric potential in the piezoelectric solid and the vector field $\mathbf{u}_m$, describing the mesh displacement with respect to the mesh domain Ω_{mo} which is regenerated at each remeshing. The equations of the problem consist of two equations for the fluid, the balance of forces and the conservation of mass, one for the solid, the balance of forces, one additional for the piezoelectric

Excerpt from the Proceedings of the 2018 COMSOL Conference in Lausanne

solid, the Gauss's Law and a last one for the mesh displacement in the mesh domain usually taken as a Poisson's like equation [9]:

$$\begin{aligned}
\rho_f \dot{\mathbf{v}}_f + \rho_f (\nabla \mathbf{v}_f)(\mathbf{v}_f - \dot{\mathbf{u}}_m) &= \operatorname{div} \Gamma \quad \text{in } \Omega_m \times \mathscr{T}, \\
\operatorname{div} \mathbf{v}_f &= 0 \quad \text{in } \Omega_m \times \mathscr{T}, \\
\rho_s \ddot{\mathbf{u}}_s &= \operatorname{div} \mathbf{S} \quad \text{in } \Omega_s \times \mathscr{T}, \\
\operatorname{div} \mathbf{D} &= 0 \quad \text{in } \Omega_{sp} \times \mathscr{T}, \\
\operatorname{div}(\mathbb{A} \nabla \mathbf{u}_m) &= 0 \quad \text{in } \Omega_{mo} \times \mathscr{T}.
\end{aligned} \tag{1}$$

The upper dot indicates the time derivative, ∇ the nabla operator, div the divergence operator, ρ_f the fluid mass density, Γ the fluid stress, ρ_s the solid mass density, $\mathbf{S}$ the solid reference stress, $\mathbf{D}$ the electric displacement of the piezoelectric solid and $\mathbb{A}$ the Winslow operator [9]:

$$(\mathbb{A} \nabla \mathbf{u}_m)_{ij} = A_{ijhk} (u_m)_{h,k}. \tag{2}$$

The fluid is assumed incompressible and linearly viscous with dynamics viscosity μ_f; its stress Γ is given by:

$$\Gamma = -p\mathbf{I} + 2\mu_f (\operatorname{sym} \nabla \mathbf{v}_f) - \frac{2}{3} \mu_f (\operatorname{div} \mathbf{v}_f) \mathbf{I}, \tag{3}$$

where p is the fluid pressure and $\mathbf{I}$ is the identity matrix. Both structural and piezoelectric solid are assumed to be linear elastic:

$$\mathbf{S} = \mathbf{F} \mathbf{S}^e, \tag{4}$$

with $\mathbf{F} = \mathbf{I} + \nabla \mathbf{u}_s$ the deformation gradient and:

$$\mathbf{S}^e = \frac{Y_s}{1+\nu_s} \mathbf{E} + \frac{Y_s \nu_s}{(1+\nu_s)(1-2\nu_s)} \operatorname{tr}(\mathbf{E}) \mathbf{I}, \tag{5}$$

for the structural solid Ω_{ss} and:

$$\mathbf{S}^e = \mathbb{C} \mathbf{E} - \mathbf{e}^T \mathbf{E}_{el}, \tag{6}$$

for the piezoelectric solid Ω_{sp}. In the structural solid, tr is the trace operator, Y_s and ν_s are respectively the Young's modulus and the Poisson ratio of the material, $\mathbf{E} = 1/2(\mathbf{F}^T \mathbf{F} - \mathbf{I})$ is the nonlinear strain measure (Green-Lagrange strain) with $\mathbf{F}^T$ indicating the transpose of $\mathbf{F}$. In the piezoelectric solid $\mathbb{C}$ is the stiffness tensor, $\mathbf{e}$ is the piezoelectric coupling tensor and $\mathbf{E}_{el} = -\nabla V$ is the electric field. Parameters of the geometry and the fluid are indicated in Table (1), while parameters of the solids and the non-zero components of $\mathbb{C}$ and $\mathbf{e}$ are indicated in Table (2). The electric displacement in the piezoelectric solid is given by:

$$\mathbf{D} = \mathbf{e} \mathbf{E} + k_o \mathbf{k} \mathbf{E}_{el}, \tag{7}$$

where k_o is the vacuum permittivity and $\mathbf{k}$ is the second-order tensor of dielectric relative permittivity measured at constant applied stress. System of equations (1) is supplemented with boundary and initial conditions; $\partial\Omega_{sm}$ is the interface between the solid body and the fluid, where FSI boundary conditions are posed:

$$\mathbf{T} \mathbf{n} = -\Gamma \mathbf{n}, \quad \mathbf{v}_f = \dot{\mathbf{u}}_m = \dot{\mathbf{u}}_s \quad \text{on } \partial\Omega_{sm} \times \mathscr{T}, \tag{8}$$

with $\mathbf{n}$ normal to the solid boundary and $\mathbf{T} = \mathbf{S}(\mathbf{F}^*)^{-1}$ the Cauchy stress in the solid; on the boundaries of the channel $\partial\Omega_m$ we assign a no-moving condition for the mesh:

$$\mathbf{u}_m = 0 \quad \text{on } \partial\Omega_m \times \mathscr{T}, \tag{9}$$

Nevertheless, on the channel boundaries we assign additional conditions. In particular, on the top and bottom boundaries of the channel $\partial\Omega_{mtb}$ we assign a no slip wall condition:

$$\mathbf{v}_f = 0 \quad \text{on } \partial\Omega_{mtb} \times \mathscr{T} \tag{10}$$

and on the left boundary of the channel $\partial\Omega_{ml}$ we assign a horizontal inlet fluid velocity condition:

$$\mathbf{v}_f = (1 - \exp(-t/\tau)) U f(Y) \mathbf{e}_1 \quad \text{on } \partial\Omega_{ml} \times \mathscr{T}, \tag{11}$$

with τ a characteristic time, U the steady inlet velocity and $f(Y)$ the vertical profile of the inlet flow:

$$f(Y) = \frac{(y - H/2)(y + H/2)}{(-H^2/4)}. \tag{12}$$

Finally, on the right boundary of the channel $\partial\Omega_{mr}$ we assign a outlet condition:

$$p = 0 \quad \text{on } \partial\Omega_{mr} \times \mathscr{T}. \tag{13}$$

At the interface between the piezoelectric solid and the structural solid $\partial\Omega_{spb}$ we assign a null reference electrical potential $V = 0$, while on the top boundary of the piezoelectric solid $\partial\Omega_{spt}$ we assign a potential $V = \tilde{V}$ such that it holds:

$$\int_{\partial\Omega_{spt}} \dot{\mathbf{D}} \cdot \mathbf{n} \, ds = \frac{\tilde{V}}{R} \tag{14}$$

where R is the external electrical load resistance. The left and right boundaries of the piezoelectric solid $\partial\Omega_{spl}$ are assumed to be insulated from an electrical point of view:

$$\mathbf{D} \cdot \mathbf{n} = 0 \quad \text{on } \partial\Omega_{spl} \times \mathscr{T}. \tag{15}$$

On the interface between the solid and the fixed circular constraint $\partial\Omega_{sc}$ the displacement of the solid is null:

$$\mathbf{u}_s = 0 \quad \text{on } \partial\Omega_{sc} \times \mathscr{T}. \tag{16}$$

Finally, we assign homogeneous initial conditions. All parameters of the model are listed in Tables (1, 2). Reynolds number of simulations is approximately 10^5.

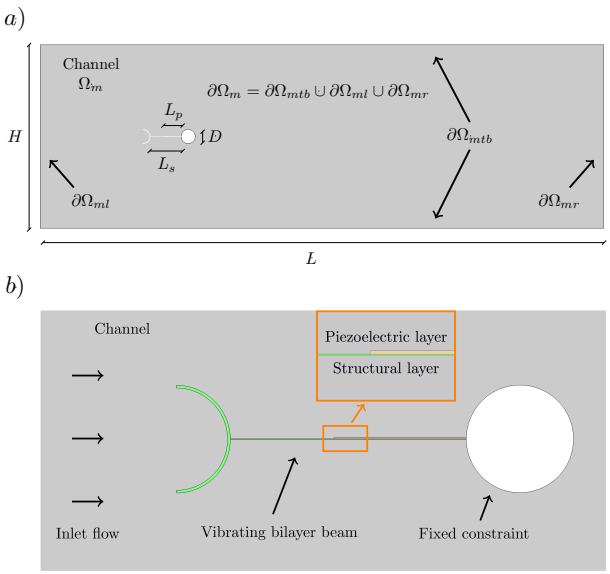

Figure 1: a) Initial geometry of the model with the boundaries of the channel where some boundary conditions are applied. The gray colored domain represents the fluid. b) Zoom of the initial geometry close to the solid. The green domain is the structural solid and the orange domain is the piezoelectric solid which is connected to an external electrical load resistance not shown in the figure.

COMSOL settings

The model is solved through a time dependent solver with a time interval from 0 to 10 s. In the time stepping node we use the backward differentiation formula (BDF) with a maximum step of 0.01 s, maximum BDF order 2 and minimum BDF order 1. Moreover, we use the PARDISO solver with the automatic (Newton) nonlinear method. The automatic remeshing feature has a distortion condition type comp1.fsi.I1isoMax<2. The model has about $3 \cdot 10^5$ degrees of freedom and takes about 2 days to run a simulation with a processor 2.3 GHz and RAM 16 GB.

Results

By solving system eq. (1) together with boundary and initial conditions, using data of Tables (1, 2), we obtain large deformations of the solid due to the fluid kinetics energy which is converted into elastic energy of the solid. In Fig. 2, fluid pressure and vorticity fields over a region of the domain are observed at different instants. The vorticity field is evaluated by taking the third component of the curl of the fluid velocity:

$$\omega = (\nabla \times \mathbf{v}_f) \cdot \mathbf{e}_3. \tag{17}$$

In particular, a large circular vortex (see Fig. 3) is created by the presence of the half cylinder. The latter is essential

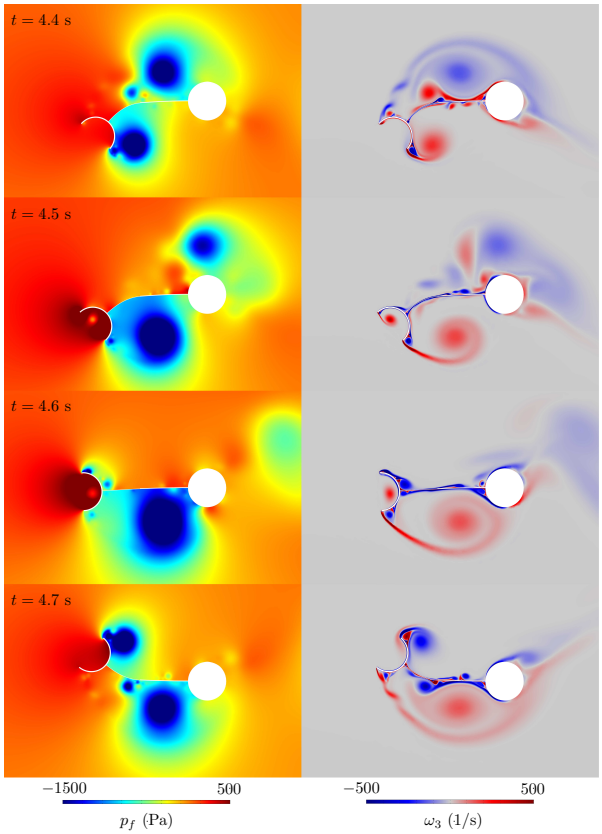

Figure 2: Pressure and vorticity fields at different instants. The solid exhibits large deformations which are described by the moving mesh and the remeshing features.

to increase vibrations of the solid and harvest more electrical power in such configuration. The pressure profile over a horizontal cut line below the solid shows a traveling wave which is not compensated by the pressure above the solid itself. This pressure difference induces a deformation which can be measured through the vertical displacement at the tip of the solid (see Fig. 4a). The displacement, after a transient state due to the evolution of the inlet profile over time, reaches a stationary oscillatory behavior. The frequency of oscillations is evaluated through a frequency spectrum showed in Fig. 4b for different inlet fluid velocities. The vibration amplitude increases with the inlet fluid velocity as showed in experimental results [5]. Moreover, also the vibration frequency reasonably increases with the inlet fluid velocity; in particular, we obtain $f = 1.4$ [Hz] and $f = 1.6$ [Hz], respectively for $U = 0.5$ [m/s] blue curve and $U = 1.0$ [m/s] red curve.

The elastic energy of the piezoelectric solid is transformed into electrical energy and harvested through an external electrical load resistance. The harvested electrical power over time is showed in Fig. 5 and evaluated by:

$$P = \frac{\tilde{V}^2}{R}. \tag{18}$$

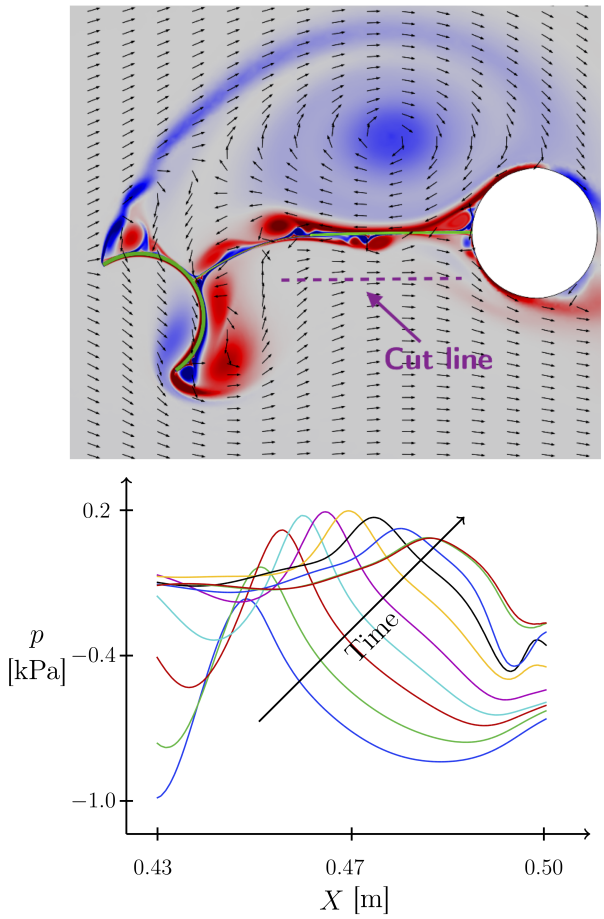

Figure 3: Top: Zoom of vorticity field and cut line where the pressure is evaluated at different instants. Bottom: Pressure is evaluated at different instants on the cut line showed in the top image. The pressure moves forward like a wave and induces large deformations of the solid.

The average harvested electrical power is approximately 0.5 [mW/m] which is in agreement with classical experimental results [2, 3]. It is worth noting, that the optimal electrical resistance load, which maximize the harvested electrical power, was not investigated in this work. Indeed, in this case, the optimal electrical resistance load depends on the vibration frequency of the solid and therefore changes with the inlet fluid velocity as demonstrated in Fig. 4. This is quite important in order to design a resistive matching circuit which optimize the energy harvesting [10].

Conclusions

We presented a model able to simulate a piezoelectric energy harvester immersed in a fluid flow. Results of simulation include: the fluid velocity and the pressure field in the channel, deformation of the solid, electrical potential in the piezoelectric solid and harvested electrical power on the external electrical load resistance. A further improvement of the model may be represented by the use of RANS-based turbulence models already implemented in COMSOL which could describe more effectively the fluid flow and its interaction with the solid.

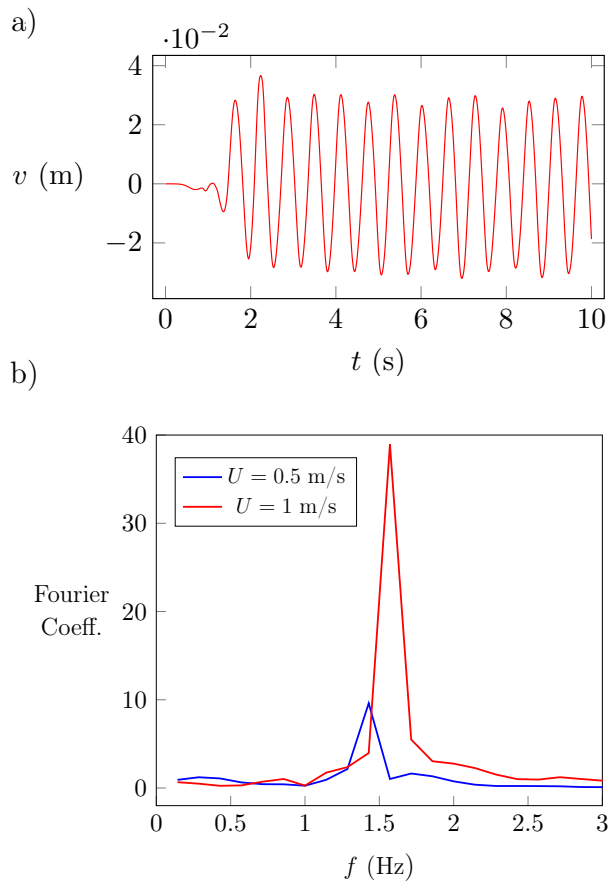

Figure 4: Vertical displacement of the solid evaluated at the free tip and its frequency spectrum. a) A stationary oscillatory movement is obtained after a transient state. b) The frequency spectrum of the vertical displacement for two different inlet fluid velocities $U = 0.5$ [m/s] blue curve and $U = 1.0$ [m/s] red curve. The peaks represent the frequencies of solid vibration.

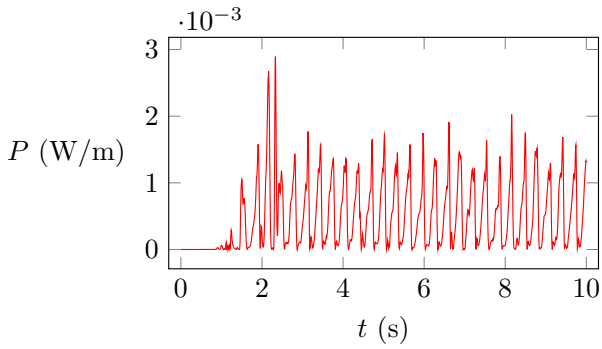

Figure 5: Harvested electrical power on load resistance over time. After the transient state, the harvested average electrical power is steady and not null.

Table 1: Geometry of the model and physical fluid parameters

L	2 [m]	channel length
H	0.65 [m]	channel height
L_s	0.11 [m]	length of structural solid
L_p	0.061 [m]	length of piezoelectric solid
h_s	$5 \cdot 10^{-4}$ [m]	structural layer thickness
h_p	$2.5 \cdot 10^{-4}$ [m]	piezoelectric layer thickness
D	0.05 [m]	fixed constraint diameter
ρ_f	1000 $[\mathrm{kg} * \mathrm{m}^{-3}]$	fluid mass density
μ_f	10^{-3} $[\mathrm{Pa} * \mathrm{s}]$	dynamic fluid viscosity
U	1 $[\mathrm{m} * \mathrm{s}^{-1}]$	fluid inlet velocity
τ_c	1 [s]	dynamic fluid viscosity

Table 2: Piezoelectric and structural solid physical parameters in the global cartesian base.

ρ_s	7800 $[\mathrm{kg} * \mathrm{m}^{-3}]$	solid mass density
Y_s	10^{11} [Pa]	Young's modulus
ν_s	0.3	Poisson ratio
$C_{11} = C_{33}$	$1.20 * 10^{11}$[Pa]	stiffness comp. 11
$C_{12} = C_{23}$	$7.51 * 10^{10}$[Pa]	stiffness comp. 12
C_{13}	$7.52 * 10^{10}$[Pa]	stiffness comp. 13
C_{22}	$1.11 * 10^{11}$[Pa]	stiffness comp. 11
$C_{44} = C_{66}$	$2.10 * 10^{10}$[Pa]	stiffness comp. 44
C_{55}	$2.25 * 10^{10}$[Pa]	stiffness comp. 55
$e_{16} = e_{34}$	12.29[C/m]	coupling comp. 16
$e_{21} = e_{23}$	-5.35[C/m]	coupling comp. 21
e_{22}	15.78[C/m]	coupling comp. 22
$k_{11} = k_{33}$	919.1	perm. comp. 11
k_{22}	826.6	perm. comp. 22

References

[1] H. A. Sodano, D. J. Inman, and G. Park, A review of power harvesting from vibration using piezoelectric materials, Shock and Vibration Digest, 36.3, 197-206, (2004).

[2] A. Erturk and D.J. Inman, Piezoelectric energy harvesting, John Wiley & Sons, (2011).

[3] S. Priya and D. J. Inman, Energy harvesting technologies. Vol. 21. New York: Springer, (2009).

[4] H. D. Akaydin, N. Elvin, Y. Andreopoulos, Wake of a cylinder: a paradigm for energy harvesting with piezoelectric materials, Experiments in Fluids, (2010).

[5] S. Orrego, K. Shoele, A. Ruas, K. Doran, B. Caggiano, R. Mittal and S. H. Kang, Harvesting ambient wind energy with an inverted piezoelectric flag. Applied Energy, 194, 212-222, (2017).

[6] M. Curatolo and L. Teresi, The Virtual Aquarium: Simulations of Fish Swimming, Proc. European COMSOL Conference, Grenoble, France, (2015).

[7] M. Curatolo and L Teresi. Modeling and simulation of fish swimming with active muscles. Journal of theoretical biology 409, 18-26, (2016).

[8] J. Donea, A. Huerta, J.-pH. Ponthot, A. Rodríguez-Ferran, Arbitrary Lagrangian-Eulerian Methods. Encyclopedia of Computational Mechanics,vol.1:Fundamentals, (2004).

[9] A. Winslow, Numerical solution of the quasilinear Poisson equations in a nonuniform triangle mesh. J. Comput. Phys. 135, 128-138 (reprint), (1997).

[10] N.A. Kong, D.S. Ha, A. Erturk and D.J. Inman, Resistive impedance matching circuit for piezoelectric energy harvesting. Journal of Intelligent Material Systems and Structures, 21(13), 1293-1302, (2010).